Experimental Investigation of Local Heat Transfer Distribution on Smooth and Roughened Surfaces Under an Array of Angled Impinging Jets[1]

Lamyaa A. El-Gabry
General Electric Company,
Global Research Center,
Niskayuna, NY 12309
e-mail: elgabry@research.ge.com

Deborah A. Kaminski
ASME Fellow
Department of Mechanical, Aerospace, and
Nuclear Engineering,
Rensselaer Polytechnic Institute,
Troy, NY 12180-3590
e-mail: kamind@rpi.edu

Measurements of the local heat transfer distribution on smooth and roughened surfaces under an array of angled impinging jets are presented. The test rig is designed to simulate impingement with crossflow in one direction. Jet angle is varied between 30, 60, and 90 deg *as measured from the target surface, which is either smooth or randomly roughened. Liquid crystal video thermography is used to capture surface temperature data at five different jet Reynolds numbers ranging between 15,000 and 35,000. The effect of jet angle, Reynolds number, gap, and surface roughness on heat transfer and pressure loss is determined along with the various interactions among these parameters.*
[DOI: 10.1115/1.1861918]

Introduction

Impingement is a common means of convectively cooling surfaces in numerous industrial applications. One such application is the cooling of gas turbine hot gas path components such as the combustion liner, transition piece, and turbine buckets and nozzles (airfoil, end wall, and shroud). Other applications for impingement include cooling of electronic components.

A two- or three-dimensional array of jets can be used for convectively cooling turbine parts. The air jets impinge at the surface to be cooled and are directed along a channel formed by the cool surface and the jet plate. In such arrangements, the downstream jets are subjected to a crossflow from the upstream jets.

There have been several experimental studies on the heat transfer characteristics of impinging jets. Researchers including Florschuetz [1–4] and Andrews [5] have studied the effect of various parameters on impingement heat transfer. Jet spacing, distance between the jet plate and target surface, and initial crossflow are among the factors studied. Tests have been conducted on staggered and inline arrays of circular jets with cossflow in single and multiple directions. Gillespie [6], Son [7], and Huang [8] used a transient liquid crystal technique for obtaining heat transfer coefficients. Gillespie [6] tested a configuration consisting of a double row of seven impingement holes exhausting through a single row of five inclined film-cooling holes. Son [7] studied the heat transfer characteristics of an impingement cooling system with uniform and nonuniform staggered array. Huang [8] conducted a detailed analysis of the heat transfer distribution under an inline array of orthogonal impinging jets. Results have shown that increasing jet Reynolds number increases the local heat transfer coefficients. Exit cross-flow direction affects flow and heat transfer distribution on the surface; the highest heat transfer coefficients were obtained for a cross-flow orientation in which the air exits from both ends of the channel that is formed by the jet plate and the target surface.

In the previously mentioned studies, jets were directed orthogonal to a smooth surface. Perry [9] studied the effect of jet angle for a single jet of hot air impinging on a surface using a water-cooled jet plate and a calorimeter to measure the impingement plate heat transfer characteristics.

Trabold [10] studied the impingement and the effect of crossflow in the presence of surface roughness elements. The surfaces were roughened with square ribs of constant rib height and varying pitch to height. Results show that roughness elements can be used to compensate for the decay in heat transfer in the cross-flow direction that is often observed with impingement on smooth surfaces.

Haiping [11] conducted an experimental investigation on the effects of certain geometric parameters including jet hole spacing, jet to surface spacing, rib pitch to height ratios, and rib height to hole diameter ratios on heat transfer. Rib roughened surfaces were also tested by Failia et al. [12]. Results show there is an optimum ratio of fin width to channel width (about one) that yields the best overall heat transfer for the lowest possible pressure requirements.

The objective of this investigation is to determine the detailed heat transfer distribution for various jet impingement configurations. The effect of randomly roughened surfaces on heat transfer is quantified and the effect of jet angle on local heat transfer distribution is determined. The use of randomly roughened surfaces provides significant heat transfer enhancement with lower pressure drops than ribbed surfaces. The method and apparatus used in these experiments are capable of reaching jet Reynolds numbers of over 35,000; this is typical of many industrial applications using jet impingement. The use of liquid crystal provides information on local heat transfer distributions.

Being able to quantify the *local* heat transfer distribution is important for two reasons. First, practical industrial experience has shown that designs that are based on average heat transfer coefficients may fail in operation due to thermal cycling and fatigue resulting from extreme temperature gradients. Another reason for measuring local distribution of heat transfer is to validate computational fluid dynamics (CFD) models used to predict heat transfer coefficients. In order to validate numerical models, it is imperative to have highly detailed experimental results.

[1]First presented at the 2001 International Mechanical Engineering Congress and Exposition of the ASME. Paper No. 2-14-1-1.

Contributed by the Turbomachinery Division of THE AMERICAN SOCIETY OF MECHANICAL ENGINEERING for publication in the JOURNAL OF TURBOMACHINERY. Manuscript received by the Turbomachinery Division December 12, 2003; revised manuscript received August 31, 2004. Associate Editor: R. S. Bunker.

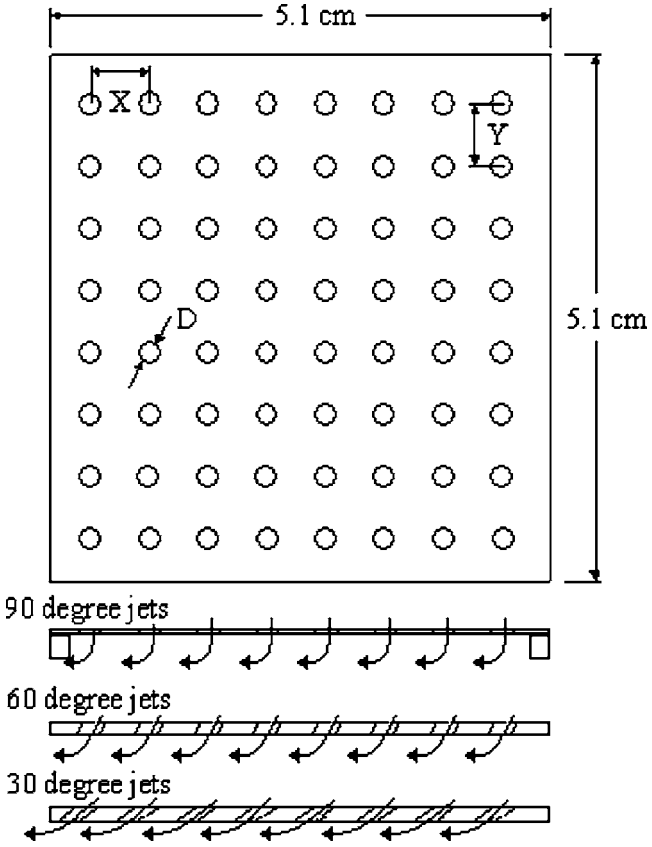

Fig. 1 Jet configuration and plate geometry

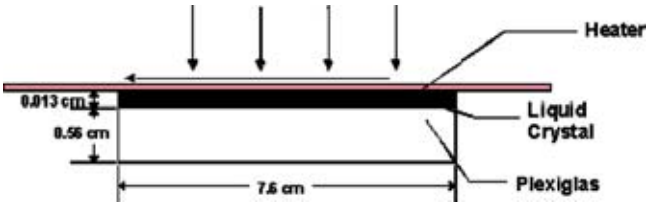

Fig. 2 Test coupon for smooth surface impingement test

Experimental Facility

Three jet plates of size 5.1 cm by 5.1 cm (2×2 in.) were tested at different Reynolds numbers ranging from 10,000 to 35,000 impinging at two channel heights. The test rig simulates impingement heat transfer with crossflow in one direction. Air is supplied to a pressure chamber (plenum). At one end of the plenum, a jet plate is mounted. Air passes from the plenum through the jet plate and impinges on either a smooth or rough surface. A passage is formed between the jet plate and the target surface by using a three-sided spacer to guide the flow to exit in one direction. There is no initial crossflow of air; the crossflow is generated from upstream rows of jets. A turbine nozzle uses this type of cooling configuration.

The holes of the jet plate were laid out in a square array as shown in Fig. 1.

The hole spacing in the x and y directions are equal (i.e., $X = Y$). The centerline distance between two adjacent holes (X) and the jet diameter (D) form a single nondimensional parameter, X/D. The gap height was also nondimensionalized with respect to jet hole diameter (Z/D). The jet diameter was 1.27 mm (0.05 in.), the spacing between jets was 6.35 mm (0.25 in.), and the height of the channel or gap was 1.27 mm (0.05 in.) and 2.54 mm (0.1 in.). The jet plates, shown in Fig. 1, are characterized by a ratio (X/D) of 5. The nondimensional parameter Z/D was set to 1 and 2 for the configurations tested.

Figure 2 is an illustration of the test coupon that consists of a target surface, heater, liquid crystal, and Plexiglas insulation. The surface is heated using a thin Inconel foil heater 0.0254 mm (0.001 in.) in thickness. This provides a constant heat flux boundary condition. Since the heater is very thin and highly conductive, the temperature across the thickness of the heater is considered negligible. In testing rough surfaces, a roughened test plate is mounted to the heater surface using an industrial grade adhesive material. The test plate is thicker than the foil heater and a thermal gradient across its thickness is accounted for using one-dimensional conduction. A calibrated liquid crystal sheet is mounted on the other side of the heater using the adhesive. A Plexiglas cover is placed on the liquid crystal face to allow visual observation of the temperature (color) fields of the target surface. The heat loss through the Plexiglas was estimated using a one-dimensional conduction model and was found to be less than 0.8% of the heat generated by the heater.

The rough surface test coupons were created using a brazing process developed by the GE Global Research Center [13]. The surface roughness was measured using a profilometer at several locations; the average roughness value was R_a of 33 μm and R_z of 179 μm. The roughness was uniform sandpaper like roughness. A photograph of the rough surface details is shown in Fig. 3.

The entire rig including plenum, jet plate, test plate, heater, liquid crystal, and Plexiglas is placed in a pressure vessel or enclosure as shown in Fig. 4. This allows control of the pressure ratio across the jet plate and, hence, allows the tests to be run at higher jet Reynolds numbers than would be possible if the air discharged to the atmosphere directly. The pressure chamber is equipped with a transparent pressure window for viewing the liquid crystal image. An RGB camera is used to grab images through the pressure window using a Data Translation DT-2871™ frame grabber. Fiber optic lighting is adjusted to provide an image of adequate quality for processing. The lighting is maintained constant throughout the experiments.

The air flow rate is measured using a venturi calibrated to ±0.5% reading located in the air supply system as described by El-Gabry [14]. The tests were run at a pressure ratio of about 1.17 that is close to the operating conditions in gas turbine applications. The chamber pressures and temperatures were measured and the flow function for each jet plate configuration was calculated.

Fig. 3 Test coupon for smooth surface impingement test (13.28×; average bump diameter ~0.25 mm)

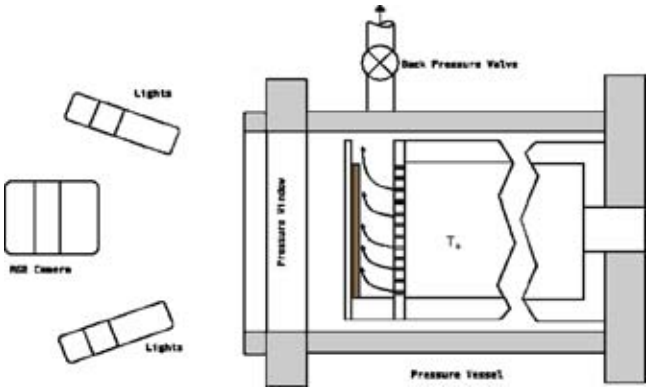

Fig. 4 Test rig in pressurized enclosure

Table 1 Average flow function for test case

	Jet angle	Z/D	Surface	Flow function[a]
1	90	2	Smooth	0.0412
2		2	Rough	0.0412
3		1	Smooth	0.0294
4	60	2	Smooth	0.0473
5		2	Rough	0.0476
6		1	Smooth	0.0393
7	30	2	Smooth	0.0460
8		2	Rough	0.0469
9		1	Smooth	0.0390

[a]Flow function is a mass flow parameter with units of $\sqrt{kg/N}$. An alternative would be to compute an effective area, which would be dimensionless. The area ratio equation can be found in Ref. [16], p. 86.

Liquid Crystal Calibration. In order to apply the "multicolor" liquid crystal technique used in this investigation, it is necessary to calibrate the liquid crystal. The calibration apparatus consists of an insulated metal bar which is heated at one end and cooled at the other thereby applying a temperature gradient to the liquid crystal sample. Thermocouples are embedded at equal distance along the calibration apparatus where the liquid crystal strip is located. As the liquid crystal temperature drops, the colors of the liquid crystal progress in this order: clear-red-yellow-green-blue-violet-clear. The clear color occurs when the temperature is outside the range of the liquid crystal. In this experiment, Hallcrest Liquid Crystal™ R40C5W is used which has a "red start" temperature of 40°C with a temperature band of 5°C. The colors of the liquid crystal are correlated to the temperatures measured by the embedded thermocouples.

Data Collection and Reduction. To collect data, the airflow rate and pressure ratio are set to the desired point to yield a given Reynolds number. Once the Reynolds number is set, a constant heat flux is applied to the target surface and once steady state has been reached, the image is captured and saved. The system has reached steady state when the liquid crystal temperature does not change more than 0.1°C over a 15–20 min interval.

In general, surface temperature variations are greater than the bandwidth of the liquid crystal (5°C) and, hence, several images need to be taken at various heat flux levels in order to get a color change in each element of the liquid crystal. These images are then superimposed and averaged to yield the heat transfer distribution on the entire surface. This process assumes that the heat transfer coefficient is not a function of heat flux making it possible to obtain an overall heat transfer coefficient distribution by averaging the partial distributions of the individual images. Details on the data reduction method using broadband steady state liquid crystal are in El-Gabry [14].

Results and Discussion

A study of the repeatability of the results was performed using one of the jet plate configurations. This study involved repeating heat transfer measurements three times at different times of day on two different days using the same jet plate. Measurements were taken using this jet plate at a jet Reynolds number of approximately 19,000. Several factors can potentially influence the experimental results. These include variation in compressor setting, ambient conditions, the lighting on the liquid crystal, the camera setting with respect to the image, and the performance of the pressure transducer. In this study, these aspects of the experimental setup were varied in order to determine the sensitivity of the results to these experimental noise parameters. The study showed that Nusselt number results for this typical plate are repeatable to within a standard deviation of 0.37 (the mean Nu for the jet plate was 79). Using the mean and standard deviation as well as some statistical relationships found in Johnson [15], one can assert with 95% confidence that at least 99% of all data obtained by repeating the test procedure described earlier will fall within 1.50 Nusselt number. This is equivalent to an error of +/−1.92% in Nusselt number using the statistical approach described in Johnson [15, p. 531] where "error" is defined in terms of deviation from the mean.

Flow Results. The flow function for each jet plate configuration was calculated to determine the effect of angle, gap height, and surface roughness on flow. This parameter is similar to the mass flow parameter defined in Shapiro [16]:

$$\text{Flow function} = \frac{\dot{m}}{A} * \frac{\sqrt{T_0}}{P_0} * \sqrt{\frac{(k-1)R}{2gk}}$$

The flow function characterizes the resistance of a flow circuit. It is commonly used in the gas turbine industry when working with impingement and orifice systems or in studying turbine blade cooling circuits from a flow effectiveness perspective. The flow function indicates the pressure needed to drive a given flow rate of air through the impingement jet plate and the cross flow channel. The higher the flow function, the lower the force needed to drive air through the system. Table 1 is a summary of the average flow functions for each configuration tested.

Flow results show that orthogonal jets have a lower flow function than angled jets regardless of surface roughness or impingement gap height. This means that the driving forces needed to flow air through the orthogonal jet plate are higher. Decreasing the gap between the jet plate and the target surface decreases the flow function (i.e., increases the driving forces needed to push air through the system). The addition of surface roughness did not measurably increase pressure drop. One explanation for this observation is that in impinging flows, the pressure drop across the jet plate (essentially an array of orifices) is greater than that through the channel. Hence, the contribution of surface roughness to overall pressure loss is small when compared to the contribution of the jet plate.

Heat Transfer Results. The local surface heat transfer coefficient is nondimensionalized using the thermal conductivity of coolant air and the jet diameter as the characteristic length. The dimensionless Nusselt number is defined as

$$\text{Nu} = hD/k_{\text{air}}$$

The conductivity of air is a function of the measured bulk fluid temperature in the plenum. The local heat transfer coefficient is defined in terms of the net heat input to the target surface and the temperature difference between the gas temperature in the plenum and the target surface temperature (derived from liquid crystal). The net heat input is equal to the heat generated by the heater less the heat lost through the Plexiglas insulator. The heat transfer coefficient is

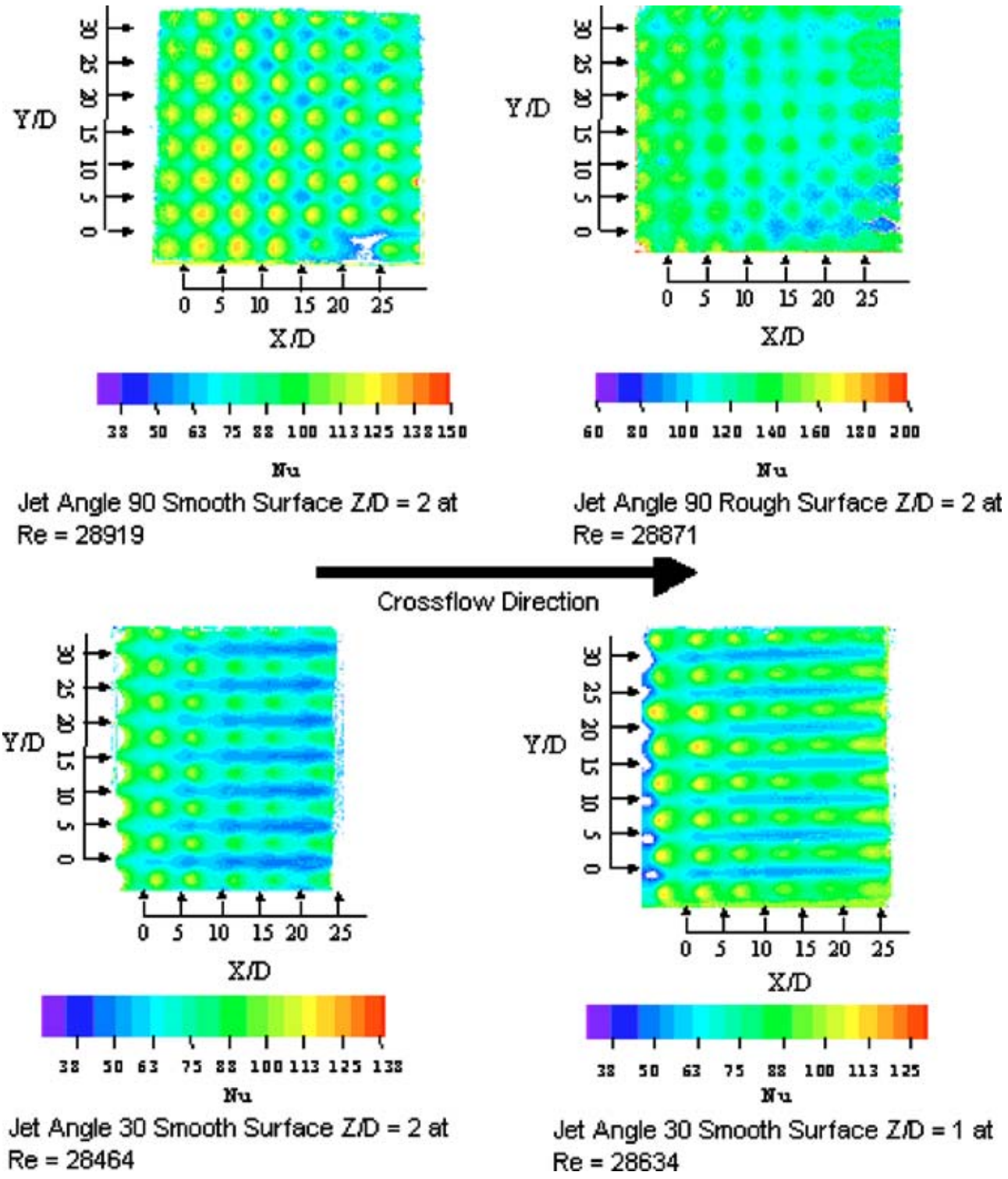

Fig. 5 Contour plots of Nusselt number distribution for various jet plate configurations

$$h = (Q_{\text{net}}/A_{\text{heater}})/(T_w - T_0)$$

The uncertainty in Nusselt number is approximately 5–10% using the method of Kline and McClintock [17].

Results show that the local Nusselt number decreases in the cross-flow direction. Figure 5 shows the Nusselt number contour plots for various configurations. Note: the Nusselt number scale is not identical for each of the contour plots in Fig. 5. A single scale cannot capture the variations in results.

In general, the highest local heat transfer is farthest from the outlet and decreases in the discharge direction. The images also show that the regions between rows of jets have lower Nusselt numbers (represented by blue on the color scale) suggesting that inline array of jets may have limited capability of uniformly cooling a surface. The angled jets yield Nusselt number distributions that appear streaked; beneath the row of jets is a strip of high heat transfer and between the rows is a strip with low heat transfer. For the orthogonal jets, there are no distinct strips with low and high heat transfer; rather there are circular regions of high heat transfer beneath the jets that extend radially outward forming smaller regions of low heat transfer between jets.

The rough surfaces exhibit a more uniform heat transfer distribution than smooth surfaces independent of jet angle.

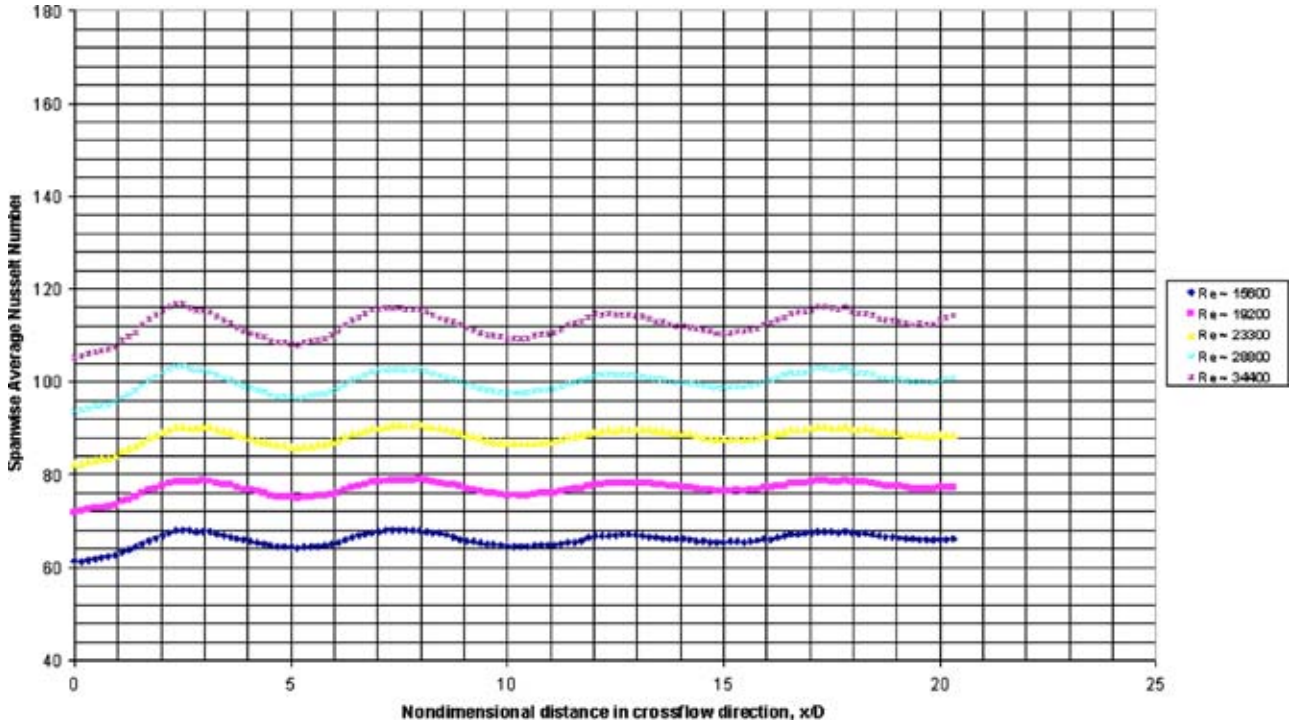

Fig. 6 Nusselt number results for 30 deg jets impinging on rough surface at gap height *Z*/*D* of 2

The spanwise averaged Nusselt number as a function of nondimensional distance in the crossflow direction (X/D) for the various test configurations are shown in Figs. 6–14. Each point in the figures represents an average of Nusselt numbers derived for all pixels at a particular X/D location. Generally peaks are near the x-location where there is a row of jets discharging fresh air into the flow stream and minima are near the x-location midway between two adjacent rows of jets.

Figures 6–8 show the Nusselt number results for configurations using the 30 deg angled jet plate. A comparison of Figs. 6 and 7 shows the effect of surface roughness on Nu number for the 30 deg jet plate. Roughness increases the average Nu and yields a more uniform heat transfer distribution; there is less decay of Nu in the cross-flow direction (increasing x/D).

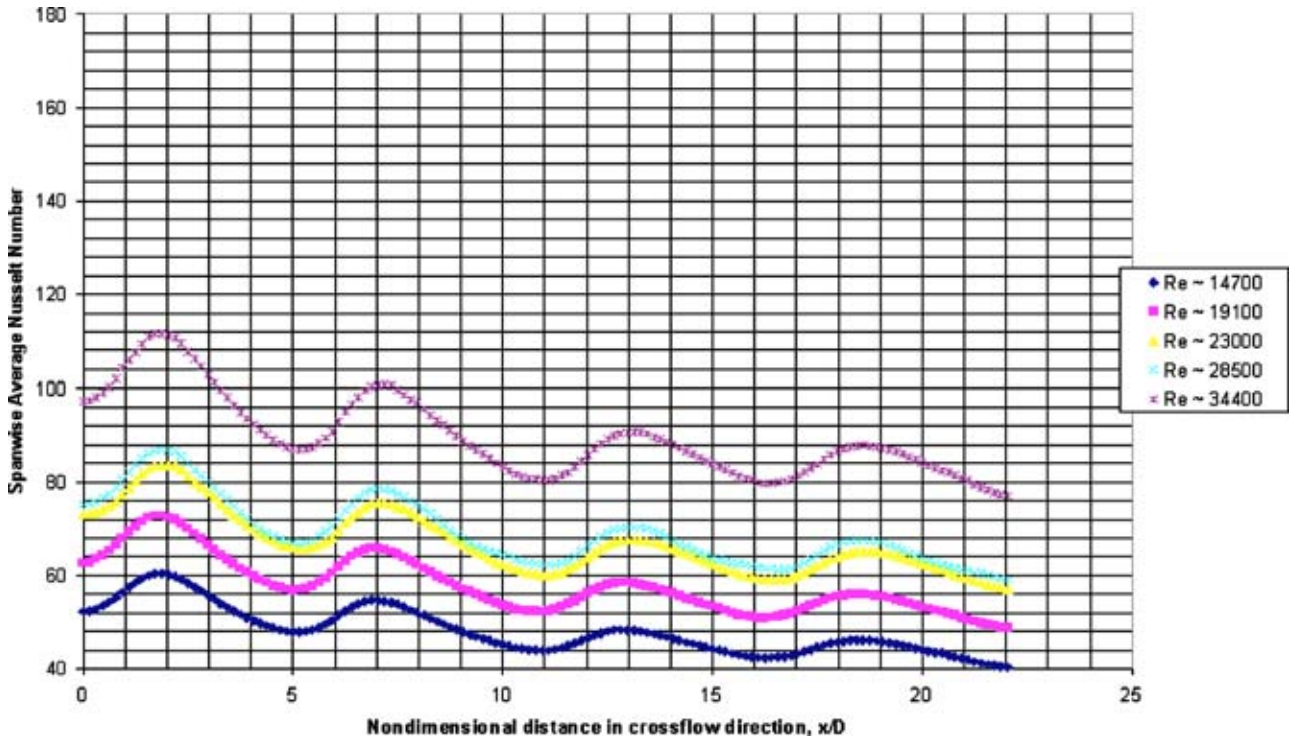

Fig. 7 Nusselt number results for 30 deg jets impinging on smooth surface at gap height *Z*/*D* of 2

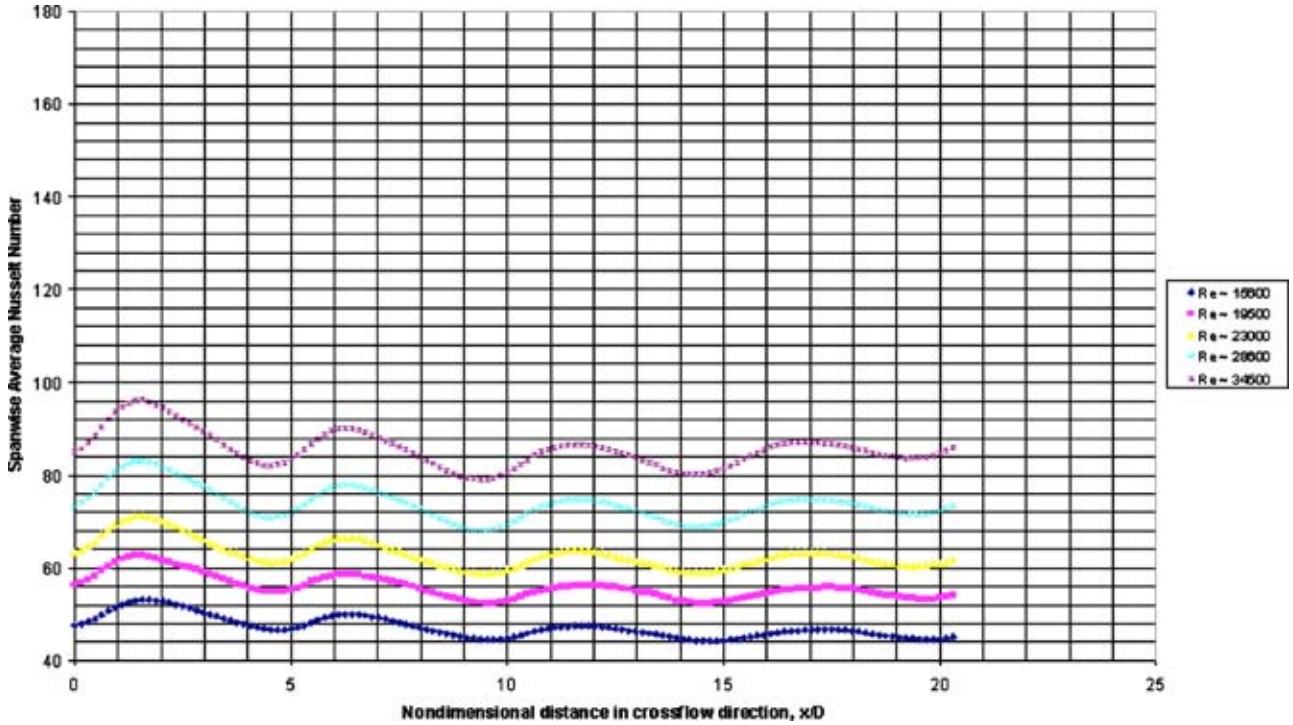

Fig. 8 Nusselt number results for 30 deg jets impinging on smooth surface at gap height *Z*/*D* of 1

At the smaller gap height (Fig. 8), the difference between neighboring maxima and minima in Nu appears lower than that for the larger gap height (Fig. 7). This is particularly evident at lower Reynolds number. In general, data, which have primarily been taken for orthogonal jets, show that the heat transfer coefficients increase with decreasing gap height. The results presented here for the 30 deg jets show an opposite trend where the heat transfer coefficient is higher at the higher gap height. One reason for this observation is that at the small gap height, the flow is predominantly channel-type flow while at the large gap, the flow is more typical of a jet impinging on a surface. The impinging jet type flow yields higher heat transfer coefficients than channel flow. However, since only two levels of gap height were tested, it is not possible to draw conclusions on a general trend between

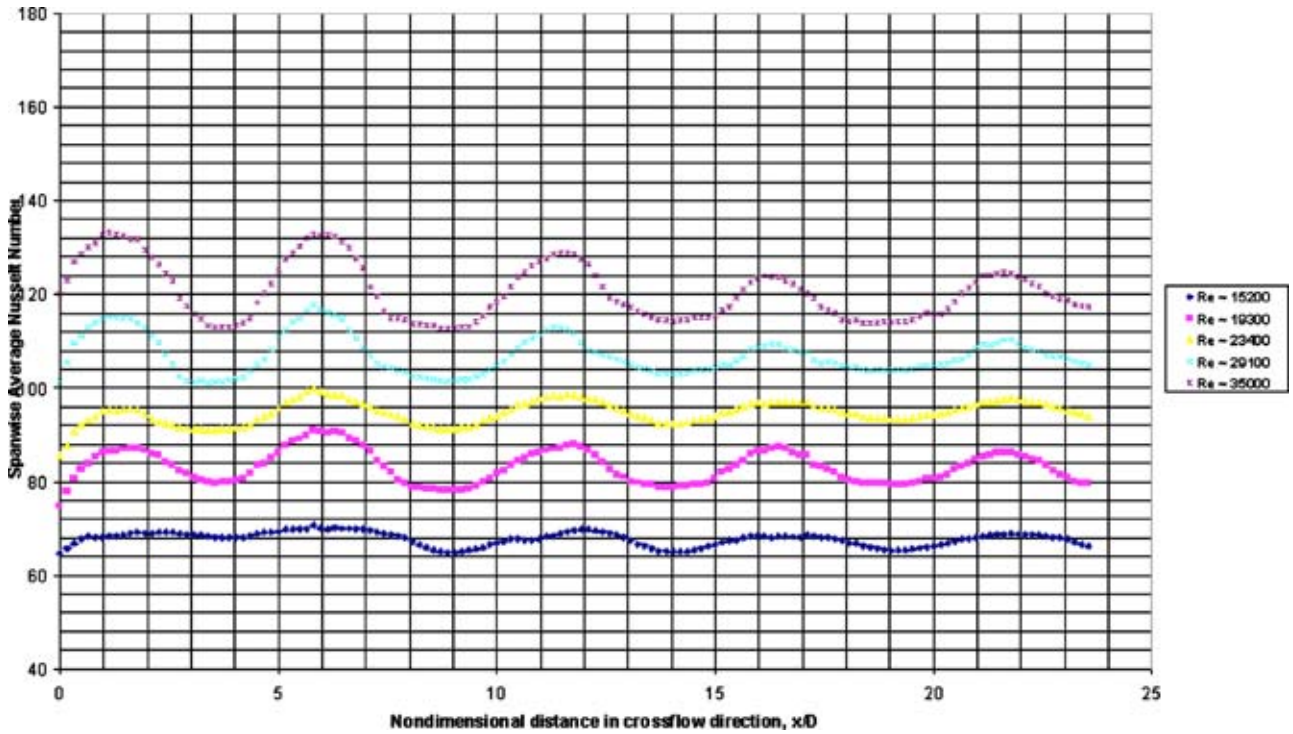

Fig. 9 Nusselt number results for 60 deg jets impinging on rough surface at gap height *Z*/*D* of 2

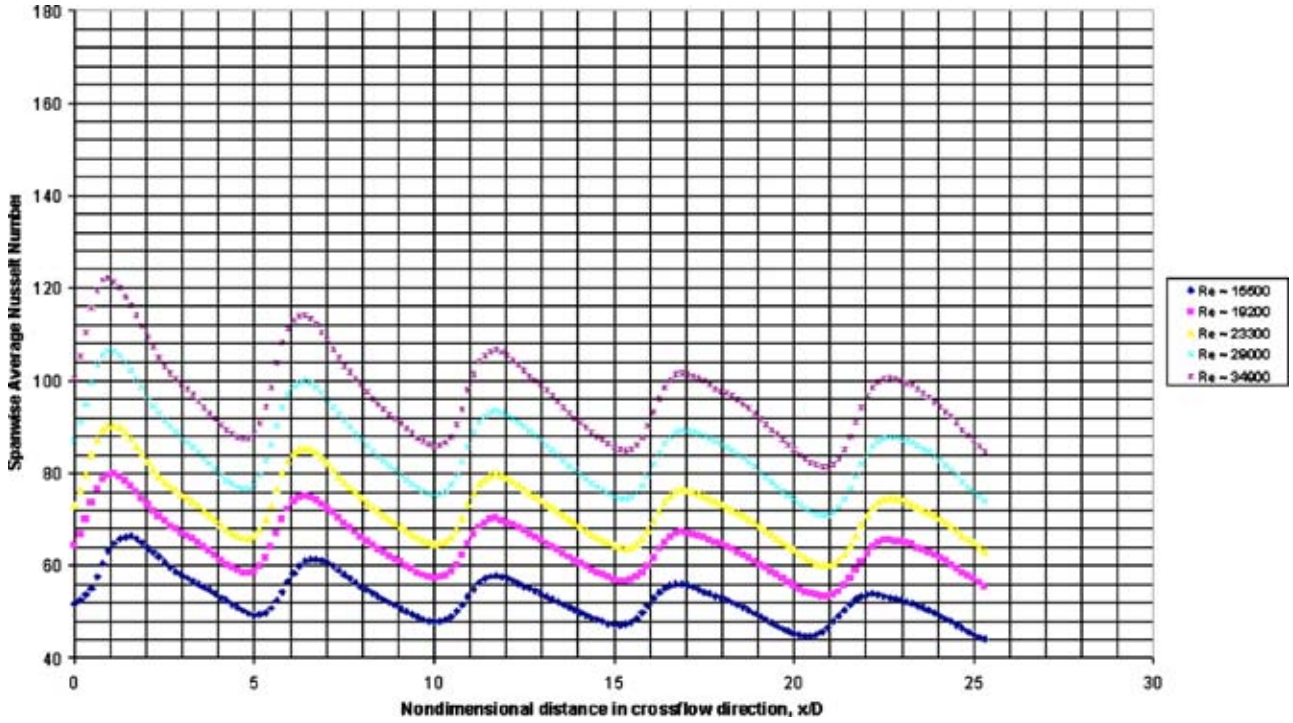

Fig. 10 Nusselt number results for 60 deg jets impinging on smooth surface at gap height *Z*/*D* of 2

gap height and thermal performance.

Figures 9–11 show the heat transfer results for the 60 deg jet plate configurations. Similar to the 30 deg jets, results from the 60 deg jets show that surface roughness increases heat transfer and yields a more uniform distribution. However, the effect of gap height is not significant to differentiate between the average heat transfer coefficients at the small and large gap heights.

Results for the 90 deg jet plate configurations are presented in Figs. 12–14. Although roughness increases uniformity of Nu on the surface, the nonuniformity is greater for the orthogonal jets than the angled jets impinging on the same roughened surface. Also worth noting is the shape of the Nusselt number distribution at the peak values (near the stagnation region). The drop in Nu on the downstream side of the stagnation region is less steep than the drop in the upstream region similar to observations reported by other researchers [3].

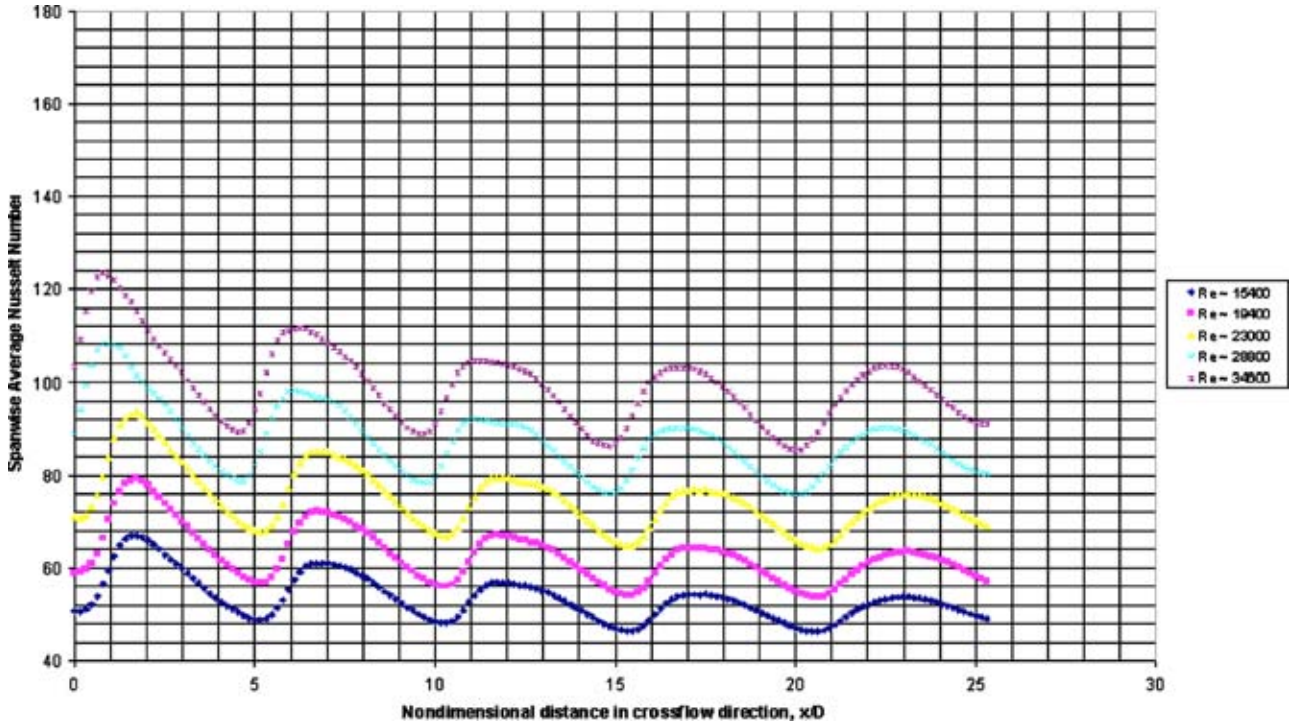

Fig. 11 Nusselt number results for 60 deg jets impinging on smooth surface at gap height *Z*/*D* of 1

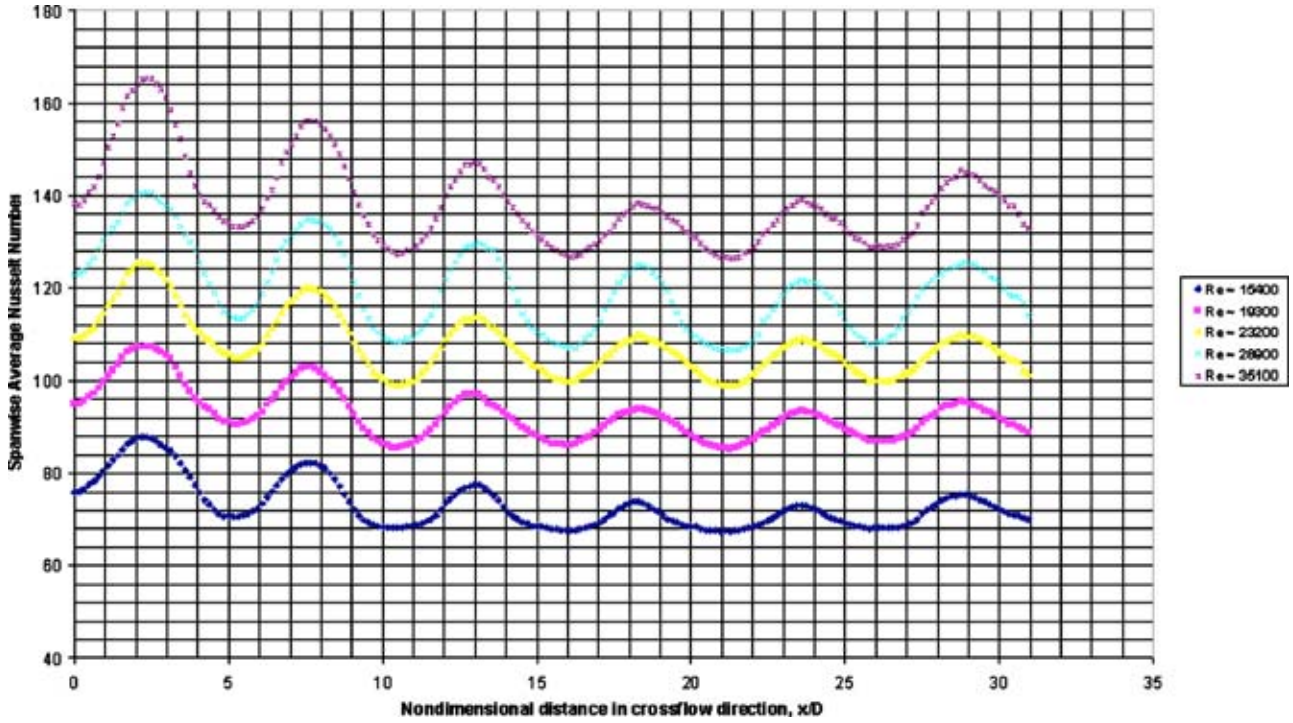

Fig. 12 Nusselt number results for 90 deg jets impinging on rough surface at gap height *Z*/*D* of 2

The results for the 90 deg jets impinging on a smooth surface at a gap height Z/D of 1 shown in Fig. 14 do not follow the same trend as other configurations; the spanwise averaged Nusselt number does not decrease in the crossflow direction. One possible explanation for this observation is that the smaller gap may be causing a large pressure drop in the channel in the crossflow direction. This pressure drop leads to nonuniform pressure drop across the jet plate in the cross-flow direction. This forces more air to flow through the jet plate holes closer to the discharge section because the channel pressure is lower in that region than it is below the upstream jet holes in the entrance region. Florschuetz et al. [2] report streamwise distribution of jet velocities for various jet plate configurations which support the results obtained for the 90 deg jet plate at $Z/D \sim 1$. For large Z/D, the jet velocities are relatively constant in the streamwise direction; however, for small Z/D, the jet velocity increases in the direction of crossflow.

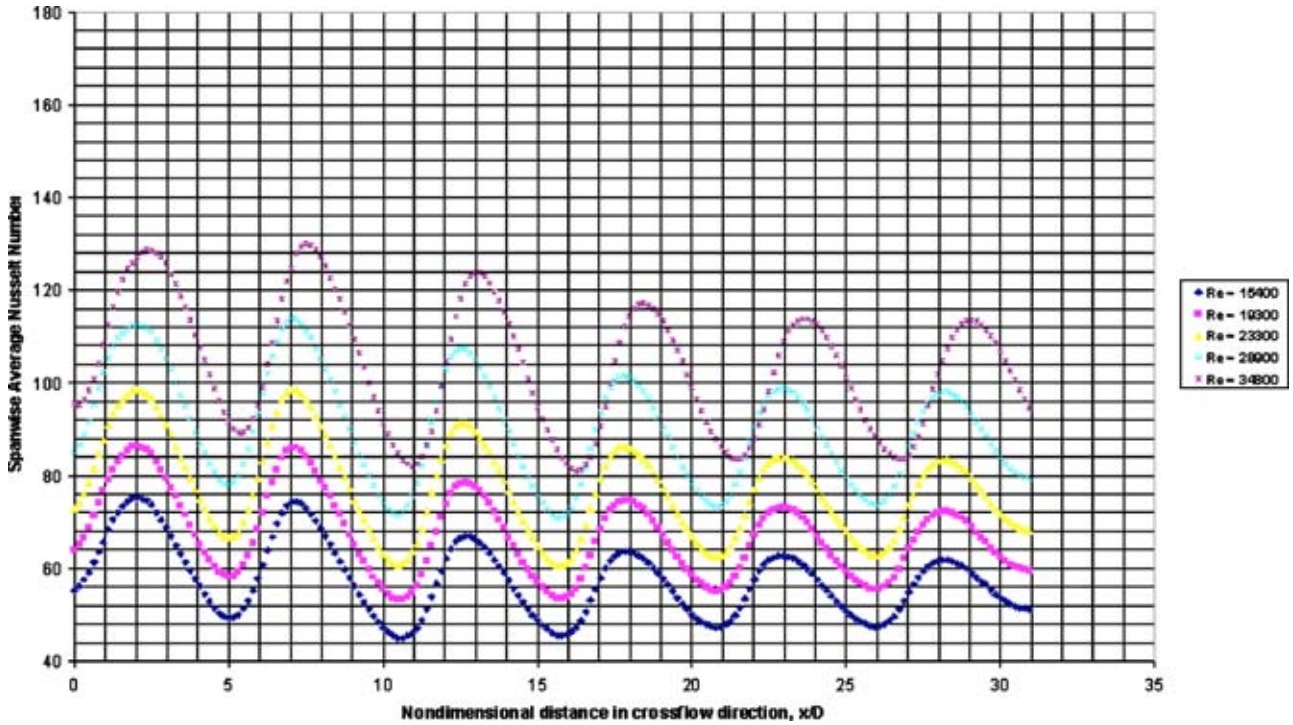

Fig. 13 Nusselt number results for 90 deg jets impinging on smooth surface at gap height *Z*/*D* of 2

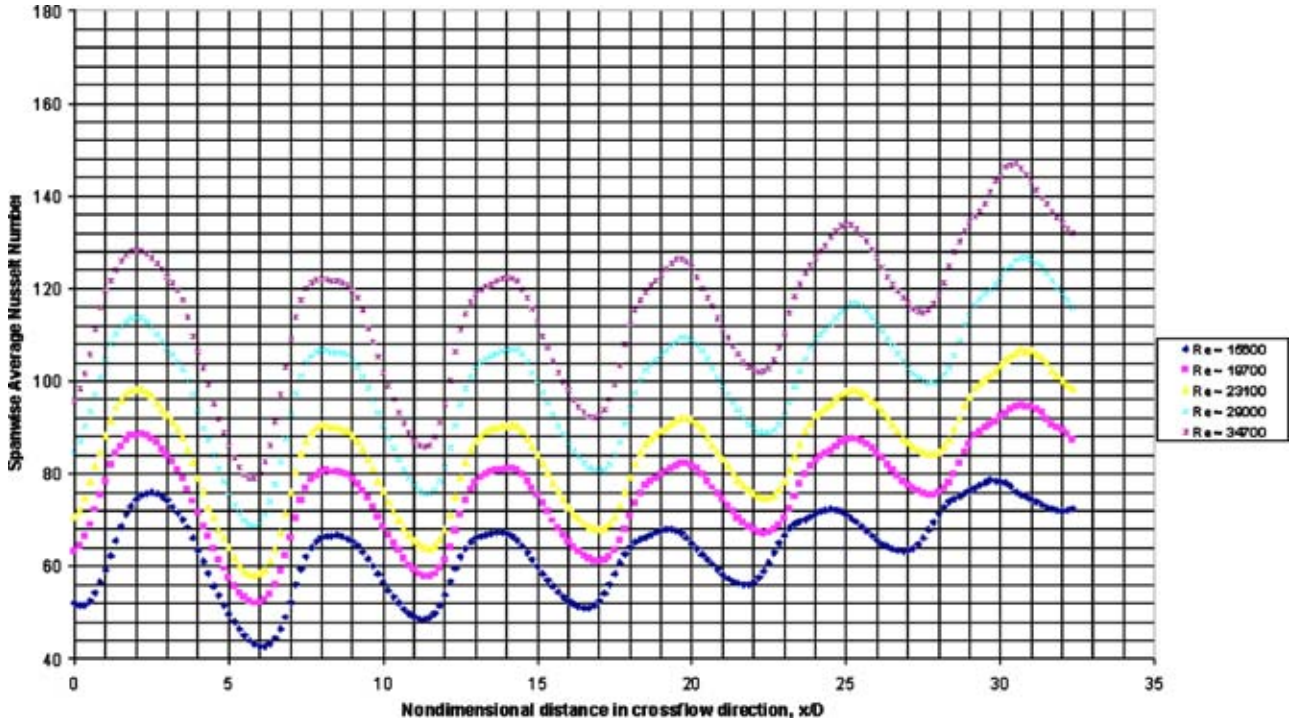

Fig. 14 Nusselt number results for 90 deg jets impinging on smooth surface at gap height *Z*/*D* of 1

Therefore, observing an increase in local Nusselt number in the cross-flow direction for the 90 deg configuration with a $Z/D \sim 1$ could be due to the increasing jet velocities.

Tables 2 shows the peak Nusselt number, average Nu, the ratio of peak to surface average Nu, and the decay rate for all test cases. Decay rate is defined as the difference between the first peak Nu (at small x/D) and the last peak Nu (at large x/D; close to discharge) divided by the first peak Nu. This definition of decay rate is used to quantify the decrease in Nusselt number in the crossflow direction as a result of the spent air heating. The results for the decay rate for the 90 deg jets impinging on a smooth surface at a gap Z/D of 1 are not shown in Table 2 because this configuration yielded results in which heat transfer was not decreasing in the crossflow direction and it is not possible to draw conclusions about decay rates.

Effect of Reynolds Number. Increasing the Reynolds number increases peak Nusselt number and average Nusselt number for all jet plate configurations. Generally, as Reynolds number increases, the peaks and troughs in the Nusselt number line plots become more defined. This means that at low Reynolds numbers, the Nusselt number distribution is more uniform.

Reynolds number appears to have no impact on decay rate; however, the amount of decay in terms of difference between first and last peak increases with increasing Re for various cases. For instance, Fig. 7 indicates that at the lowest Reynolds number the decay rate is about 23.8% while at the highest Reynolds number it is 21.1% and the trend is that decay rate decreases with increasing Reynolds number. However, the actual decay in terms of the difference between the first and last peak Nu values is 14.4 for the lowest Re and 23.6 for the highest Re; therefore, the amount of decay in Nusselt number increases with increasing Reynolds number.

The effect of crossflow is to decrease Nu in the direction of spent airflow; increasing Reynolds number increases the heat transfer coefficients at the stagnation region and also increases the amount by which Nu decays as measured from neighboring peak to valley.

Effect of Jet Angle. The surface average Nusselt number increases with increasing jet angle, as does the peak Nusselt number, independent of gap height, surface roughness, and Reynolds number. This is to be expected because when the jet is directed orthogonal to the surface, it can pickup the most heat upon striking the surface. Increasing the angle increases the stagnation point heat transfer.

Effect of Gap Height. Figure 15 shows the effect of gap height on surface average Nu. Increasing gap height decreases both peak and average Nusselt numbers for the 90 deg array of jets. The effect is not as significant for the 60 deg jets and for the 30 deg jets, the average Nusselt number increases with increasing gap height.

Effect of Roughness. For any given jet Reynolds number, roughness increases the average Nu for all jet plates tested regardless of jet angle as shown in Fig. 16. Note the highest surface average Nu obtained with a smooth surface is lower than the lowest average Nu obtained with a roughened surface for any given jet Reynolds number. A comparison of the top two contour plots in Fig. 5 for the 90 deg smooth and rough surfaces demonstrates the effect of roughness; the rough surface shows higher and more uniform heat transfer. A comparison of Figs. 6 and 7 for the 30 deg jets, Figs. 9 and 10 for the 60 deg jets, and Figs. 12 and 13 shows that roughness has the same effect of yielding increased, uniform heat transfer independent of jet angle.

Comparison with Existing Data. In the literature, there are heat transfer results for arrays of jets impinging orthogonal to a flat smooth surface. The surface average Nusselt number for the orthogonal jets was compared with data tabulated in the NASA CR 3217 [18] and with the predicted values using an empirical relation posed by Kercher and Tabakoff [19] for a square array of circular jets impinging orthogonal to a flat smooth surface.

The average Nusselt number as a function of Reynolds number is plotted for Z/D of 1 and 2. The results, shown in Fig. 17, are close to published values. Note, however, that the effect of Z/D is

Table 2 Nusselt number results of interest

Jet angle	Gap height Z/D	Surface	Jet Re	Peak Nu	Aug Nu	Peak/avg	Decay rate (%)
30	2	Rough	15600	68	66.04	1.030	2.9
			19200	79	77.02	1.026	2.5
			23300	91	88.39	1.030	2.9
			28800	104	99.95	1.041	2.9
			34400	117	112.42	1.041	2.6
30	2	Smooth	14700	60.4	48.2	1.253	23.8
			19100	72.8	57.9	1.257	23.1
			23000	83.8	67.1	1.249	22.4
			28500	86.9	69.2	1.256	21.7
			34400	111.6	89.8	1.243	21.1
30	1	Smooth	15600	53.1	47.2	1.125	13.4
			19500	62.7	55.9	1.122	10.7
			23000	71.3	63.1	1.130	10.2
			28600	83.2	73.8	1.127	8.7
			34500	96.3	85.7	1.124	8.6
60	2	Rough	15200	70.7	67.8	1.043	3.8
			19300	91	83.1	1.095	5.5
			23400	99.8	94.8	1.053	2.8
			29100	118	107	1.103	6.8
			35000	133	120.6	1.103	6.8
60	2	Smooth	15500	66.3	53.1	1.249	18.6
			19200	79.8	64	1.247	17.3
			23300	90.3	72.5	1.246	16.9
			29000	106.4	85	1.252	17.3
			34900	112.1	96.9	1.157	9.0
60	1	Smooth	15400	67.1	53.5	1.254	19.5
			19400	79.3	62.7	1.265	19.3
			23000	93.6	74.9	1.250	18.8
			28800	108.1	87.5	1.235	16.7
			34600	123.4	99.4	1.241	15.7
90	2	Rough	15400	88	73.2	1.202	15.9
			19300	107.3	92.8	1.156	12.4
			23200	125.5	107.9	1.163	12.4
			28900	140.5	119.7	1.174	13.2
			35100	165.5	138.4	1.196	15.4
90	2	Smooth	15400	76	57.6	1.319	18.4
			19300	86	67.2	1.280	16.3
			23300	99	77.2	1.282	15.2
			28900	112	90.3	1.240	11.6
			34800	129	103.8	1.243	11.6
90	1	Smooth	15600	78.7	63.2	1.246	
			19700	94.8	75.5	1.256	
			23100	106.9	84.4	1.267	N/A
			29000	126.7	99.9	1.268	
			34700	147.1	114.8	1.281	

not as pronounced in the Florschuetz data as it is in the experimental results obtained in this study. Also note that this study used square arrays of jets, however, the data reported by Florschuetz et al. [16] used rectangular arrays where the Y/D was 4; the X/D spacing is the same for both sets of data. Another difference between the two data sets was in how the heat transfer coefficient was obtained; Florschuetz used a series of embedded thermocouples to measure the surface temperature, this study used liquid crystals to get a more detailed description of the temperature. The results obtained from the correlation proposed by Kercher et al. [19] suggest that the average Nu is higher for the larger gap than the smaller gap. The difference, however, between the average values predicted by Kercher at $Z/D=1$ and $Z/D=2$ is small (about 6.5%) and may be statistically insignificant considering experimental uncertainty and the variance between Kercher's data and the curve fit used in developing the correlation.

In addition to the comparison of overall average Nu, an attempt was made to compare spanwise average Nu results obtained in this experiment with predicted spanwise values using the correlation proposed by Florschuetz et al. [2]. Results were compared at the highest and lowest jet Reynolds numbers for both Z/D heights; in all, four comparisons were made. The results of the comparison at the low Re are shown in Fig. 18.

The agreement in Nu is fair. In cases where the predicted Nu does not match the measured Nu, the trend in streamwise direction is the same. For the smaller Z/D, both the test data and Florschuetz correlation show that Nu does not decay in the streamwise direction for the entire length of the passage. The differences between the measurement techniques used by the authors may contribute to the differences in results. The correlation yields a spanwise average Nu as a function of row number; hence, one has a single discrete Nu value for each row. The liquid crystal technique results in a more continuous detailed stream of data results. Therefore in order to compare test results with the correlation, it was necessary to subdivide the test results (such as those shown in Fig. 6) into subsections and average over the entire subsection to obtain a value comparable to the "row" value that the correlation would yield. This process in itself may cause some differences.

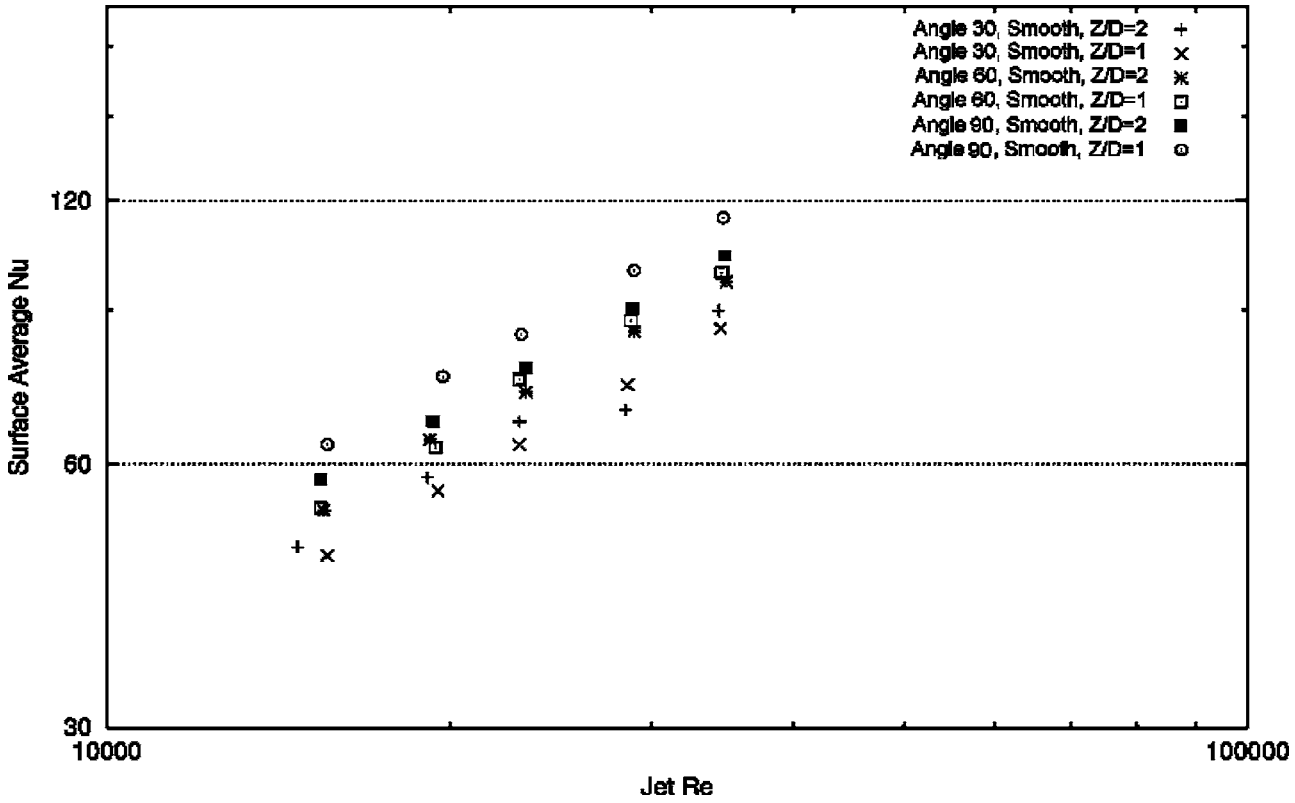

Fig. 15 Effect of gap height Z/D on average Nusselt number

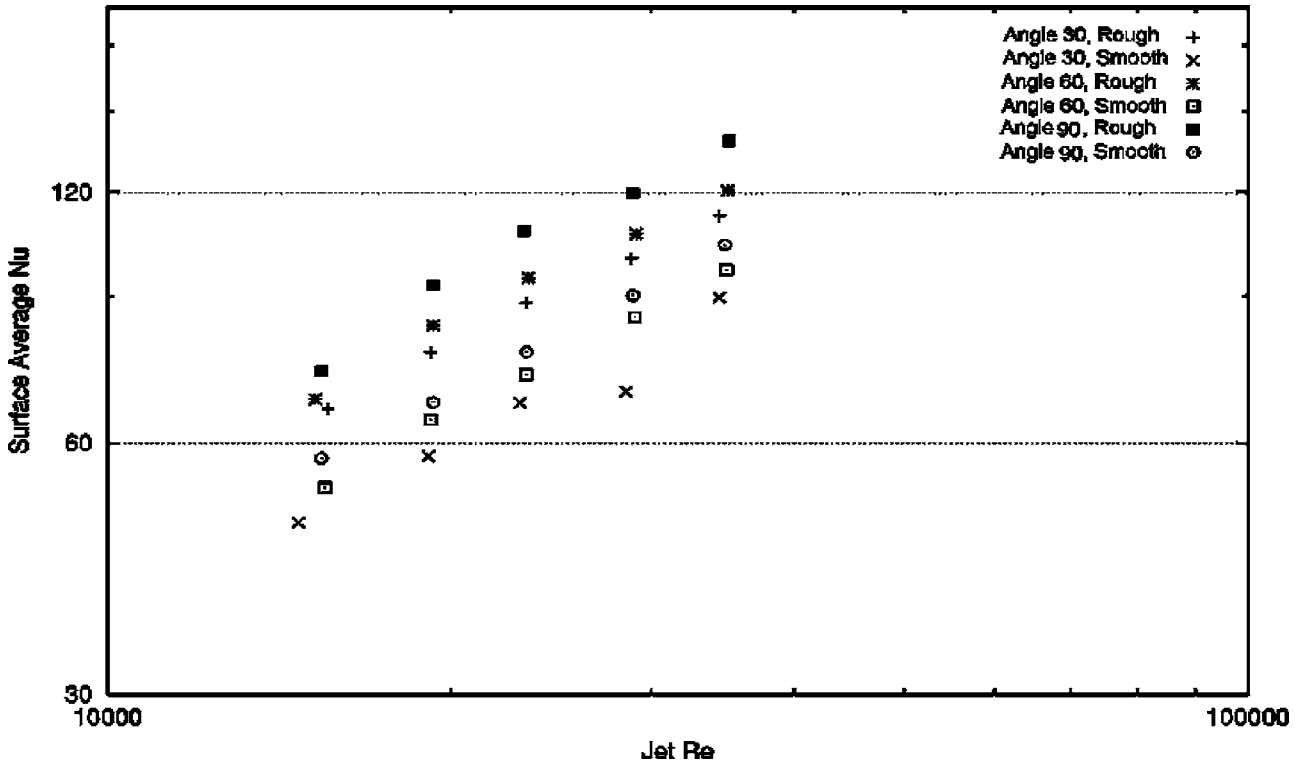

Fig. 16 Effect of roughness on average Nusselt number at $Z/D=2$

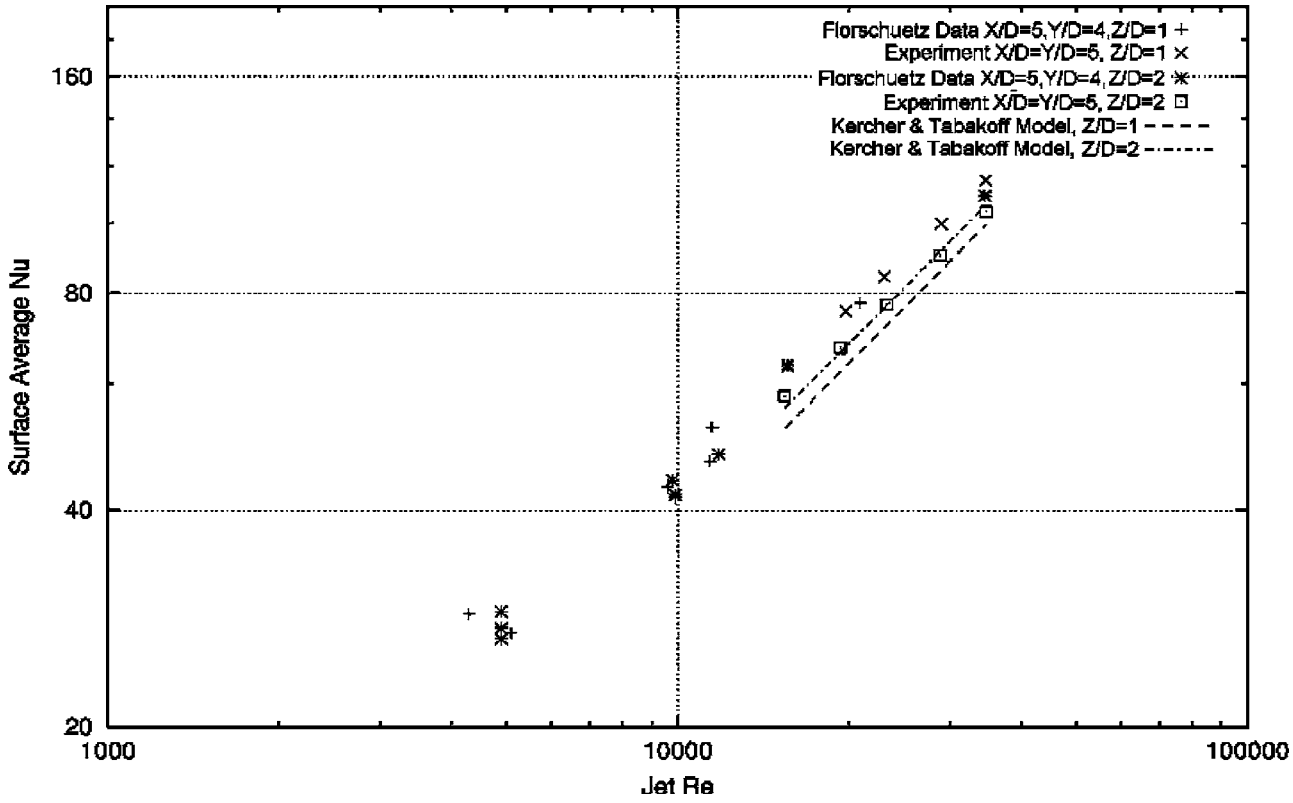

Fig. 17 Comparison of average Nusselt number for 90 deg jets with published results

Conclusions

In summary, the optimum design would utilize roughened surfaces since they enhance heat transfer significantly. Furthermore, rough surfaces reduce nonuniformity of surface temperature. Reducing nonuniformity can increase part life by reducing thermal gradients and thermal-induced stresses. The additional pressure drop due to the surface roughness is negligible when compared to the pressure drop through the jet plate. The small gap height presents a higher system pressure drop without significantly increasing heat transfer; hence, small gap heights should be avoided. Nonorthogonal jets reduce heat transfer but tend to generate more uniform heat transfer distributions. Hence, jet angle is yet another parameter that can be varied in a design to reduce thermal gradients especially when maximizing overall heat transfer coefficients is not the only important objective.

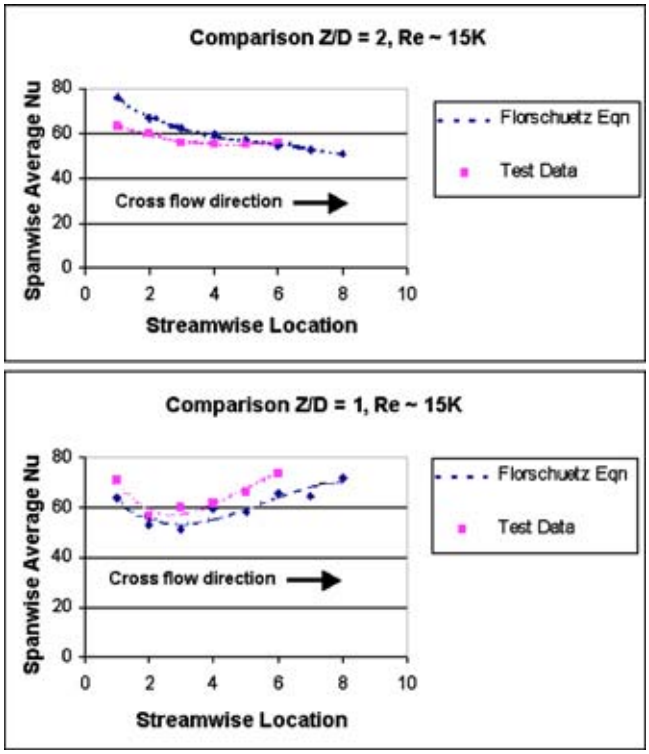

Fig. 18 Comparison of spanwise average Nusselt number for 90 deg jets

Acknowledgments

The authors would like to acknowledge N. Nirmalan, J. Bailey, R. Bunker, and S. Brzozowski at the General Electric Global Research Center for their support and insight

Nomenclature

A = flow area of array of jets
D = impingement jet hole diameter
g = acceleration due to gravity
k_{air} = thermal conductivity of air
k = specific heat ratio, Cp/Cv
$\dot{m}$ = measured mass flow rate of air
N = number of circular holes in jet plate
Nu = Nusselt number$=hD/k_{air}$
P_0 = pressure in the pressure chamber
P_{ex} = discharge pressure at exit of impingement channel
Q_{heater} = heat generated by foil heater
Q_{loss} = estimated heat loss through Plexiglas insulation
R = gas constant of air

R_a = centerline average roughness—arithmetical average value of all distances of the roughness profile from its centerline over a length of 15 mm[2]

R_z = average peak to peak roughness—average value of the greatest single peak to peak reading from five sequential lengths of 2.5 mm on the surface trace

Re = average jet Reynolds number=$4\dot{m}/\mu\pi DN$

T_0 = temperature in the plenum chamber

T_w = temperature of target surface (cold gas side)

X = stream-wise spacing of jet holes of impingement plate

Y = span-wise spacing of jet holes of impingement plate

Z = distance between the jet plate and the target surface

μ = dynamic viscosity of air

θ = jet angle (90 deg is orthogonal to the target surface)

References

[1] Florschuetz, L. W., Berry, R. A., and Metzger, D. E., 1980, "Periodic Streamwise Variations of Heat Transfer Coefficients for Inline and Staggered Arrays of Circular Jets with Crossflow of Spent Air," ASME J. Heat Transfer, **102**, pp. 132–137.

[2] Florschuetz, L. W., Truman, C. R., and Metzger, D. E., 1981, "Streamwise Flow and Heat Transfer Distributions for Jet Array Impingement with Crossflow," ASME J. Heat Transfer, **103**, pp. 337–342.

[3] Florschuetz, L. W., Metzger, D. E., and Su, C. C., 1984, "Heat Transfer Characteristics for Jet Array Impingement with Initial Crossflow," ASME J. Heat Transfer, **106**, pp. 34–41.

[4] Florschuetz, L. W., and Isoda, Y., 1983, "Flow Distributions and Discharge Coefficient Effects for Jet Array Impingement with Initial Crossflow," ASME J. Eng. Power, **105**, pp. 296–304.

[5] Andrews, G. E., and Hussain, C. I., 1986, "Full Coverage Impingement Heat Transfer: The Influent of Channel Height," *Proceedings of the 8th International Heat Transfer Conference*, Vol. 3, pp. 1205–1211.

[6] Gillespie, D. R. H, Wang, Z. Ireland, P. T., and Kohler, S. T., 1998, "Full Surface Local Heat Transfer Coefficient Measurements in a Model of an Integrally Cast Impingement Cooling Geometry," ASME J. Turbomach., **120**, pp. 92–99.

[7] Son, C., Gillespie, D., Ireland, P., and Dailey, G., 2001, "Heat Transfer and Flow Characteristics of an Engine Representative Impingement Cooling System," ASME J. Turbomach., **123**, pp. 154–160.

[8] Huang, Y., Ekkad, S. V., and Han, J., 1998, "Detailed Heat Transfer Distribution under an Array of Orthogonal Impinging Jets," J. Thermophys. Heat Transfer, **12**(1), pp. 73–79.

[9] Perry, K. P., 1954, "Heat Transfer by Convection from a Hot Gas Jet to a Plane Surface," Proc. Inst. Mech. Eng., Vol. **168**, pp 775–784.

[10] Trabold, T. A., and Obot, N. T., 1987, "Impingement Heat Transfer Within Array of Circular Jets: Part II—Effects of Crossflow in the Presence of Roughness Elements," ASME J. Turbomach., **109**, pp. 594–601.

[11] Haiping, C., Jingyu, Z., and Taiping, H., 1998, "Experimental Investigation on Impingement Heat Transfer From Rib Roughened Surface within Array of Circular Jet: Effect of Geometric Parameters," ASME Paper No. 98-GT-208.

[12] Failla, G., Bishop, E. H., and Liburdy, J. A., 1996, "Enhanced Jet Impingement Heat Transfer with Crossflow at Low Reynolds Numbers," ASME National Heat Transfer Conference, HTD-Vol. 324, pp. 107–113.

[13] Johnson, R. A., Loprinzo, A. J., Lee, C., Abuaf, N., Hasz, W. C., and Morton, L. M., 2003, "Method & Apparatus for Enhancing Heat Transfer in a Combustor Liner for a Gas Turbine." U. S. Patent No. 6,526,756 B2 (Mar. 4, 2003).

[14] El-Gabry, L. A., 2003, "Local Heat Transfer Distribution on Smooth and Roughened Surfaces under an Array of Angled Impinging Jets," Ph.D. thesis, Rensselaer Polytechnic Institute.

[15] Johnson, R. A., 1994, *Miller and Freund's Probability and Statistics for Engineers*, Prentice–Hall, Englewood Cliffs, NJ.

[16] Shapiro, A. H., 1953, *The Dynamics and Thermodynamics of Compressible Fluid Flow*, Vol. 1, Wiley, New York.

[17] Kline, S. J., and McClintock, F. A., 1953, "Describing Uncertainties in Single-Sample Experiments," Mech. Eng. (Am. Soc. Mech. Eng.), **75**, pp. 3–8.

[18] Florschuetz, L. W., Metzger, D. E., Takeuchi, D. I., and Berry, R. A., 1980, "Multiple Jet Impingement Heat Transfer Characteristic—Experimental Investigation of In-Line and Staggered Arrays With Crossflow," NASA-CR-3217, Arizona State University, Tempe, AZ.

[19] Kercher, D. M., and Tabakoff, W., 1970, "Heat Transfer by a Square Array of Round Air Jets Impinging Perpendicular to a Flat Surface Including the Effect of Spent Air," ASME J. Eng. Power, **92**, pp. 73–82.

[2]The lengths of 15 and 2.5 mm in the R_a and R_z definitions are specific to the profilometer settings.